

DEVELOPMENT OF FUEL ROD THERMAL-HYDRAULIC MODEL FOR THE THERMAL-HYDRAULIC FEEDBACK IN CONDOR CODE

Yousef I. AlZaben^a and Eduardo A. Villarino^b

^a*Nuclear Science Research Institute, King Abdulaziz City for Science and Technology, Riyadh, Saudi Arabia, yalzibn@kacst.edu.sa*

^b*Nuclear Engineering Department, INVAP S.E, Av. Cmte. Luis Piedrabuena 4950, R8403CPV, S.C Bariloche, Argentina, men@invap.com.ar*

Keywords: Finite Difference, CONDOR, XS Temperature Dependent, High Burnup, Neutronic and Thermal-Hydraulic Feedback.

Abstract. The fuel at high burnup has a complex behavior due to the resonance absorptions of the U^{238} and the Pu^{239} production especially at the rim zone of the fuel pin. For that reason, the radial dependence of the generated power and the corresponding burnup needs to be carefully studied. The resonance effects has a high dependence with temperature that depends on the generated power, hence, it needs to be properly evaluated. At the rim zone, the resonance effects dependence with fuel temperature becomes more significant than the inner zones. This fact requires a thermal-hydraulic model to take this effect into consideration as a function of burnup. Cladding temperature will be also evaluated to take care of the resonance cross section of the cladding material.

In this work, a one dimensional steady state heat equation is used to formulate a set of finite difference equations to evaluate temperature distribution in fuel pin for a non-uniform power generation. Material properties such as thermal conductivity are considered to be a function of temperature and burnup.

The model would solve pin by pin temperature distribution in a fuel assembly array for a non-uniform radial and potential azimuthal discretization. Verification against analytical solution and simple test cases are demonstrated.

The application of this work would be for BWR, PWR, CANDU, ATUCHA and TRIGA fuel pin. Upon a successful implementation of this model, it would be in future integrated with CONDOR code.

1 INTRODUCTION

Recently, there were initiatives taken toward increasing the fuel burnup in order to utilize most of its power and to reduce the depository requirements by burning the actinides. The fuel at high burnup has a complex behavior due to the resonance absorptions of the U^{238} and the production of Pu^{239} especially at the rim zone of the fuel pin. The resonance effects have a high dependence with temperature, which depends on the generated power. Thus, it requires a thermal-hydraulic feedback model to take this complex behavior into consideration.

In this paper, a one dimensional steady state heat conduction equation is formulated in its integral form to evaluate the temperature distribution in a fuel pin or plate for a non-uniform power generation. Material properties such as thermal conductivity are considered to be a function of temperature and burnup.

A set of finite difference equations were developed to solve the integral heat conduction equation. Each mesh interval may have a different spacing distance, material properties and/or power density.

The model would be used to solve pin by pin the temperature distribution in a fuel assembly array for a non-uniform radial and potential azimuthal discretization. This model would be applied for PWR, BWR, CANDU, ATUCHA and TRIGA fuel pin. Figure 1 shows an example of solid and annular fuel rod which might be considered for determining the temperature distribution.

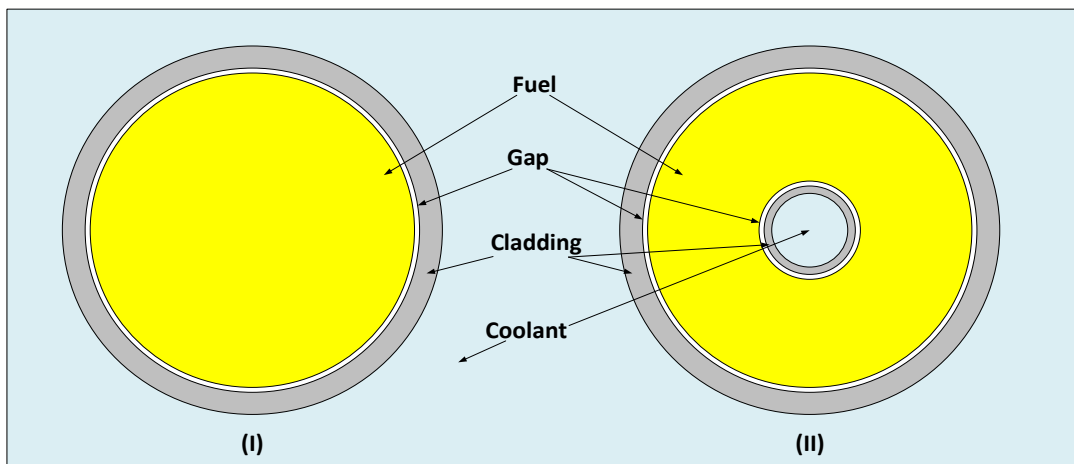


Figure 1: Models considered for determining temperature distribution, (I) solid fuel rod and (II) annular fuel rod.

2 THERMAL-HYDRAULIC MODEL

The integral form of the steady state heat conduction equation (Todreas and Kazimi, 1993), which describes the temperature distribution in a solid material, is given by:

$$-\iint_S k(\vec{r}, T) \vec{\nabla} T(\vec{r}) \cdot \vec{n} dS = \iiint_V q'''(\vec{r}) dV \quad (1)$$

Where:

k : thermal conductivity (W/m.K)

T : temperature (K)

S : surface area (m²)

q''' : power density (W/m³)

V : volume (m³)

At the exterior surfaces, a general boundary condition is applied that has the form:

$$\alpha(T) T + \beta(T) \frac{\partial T}{\partial n} = \gamma(T) \quad (2)$$

Where:

α , β and γ : material properties constants (W/m².K), (W/m.K) and (W/m²), respectively.

2.1 Numerical Modeling

The heat conduction equation is discretized using the finite difference method (FDM). In order to be able to apply FDM, the thermal conductivity and power density were assumed to be spatially constant over each mesh interval. The temperature gradient was simplified by a first order difference. Figure 2 shows the mesh point layout used to solve for the temperature distribution.

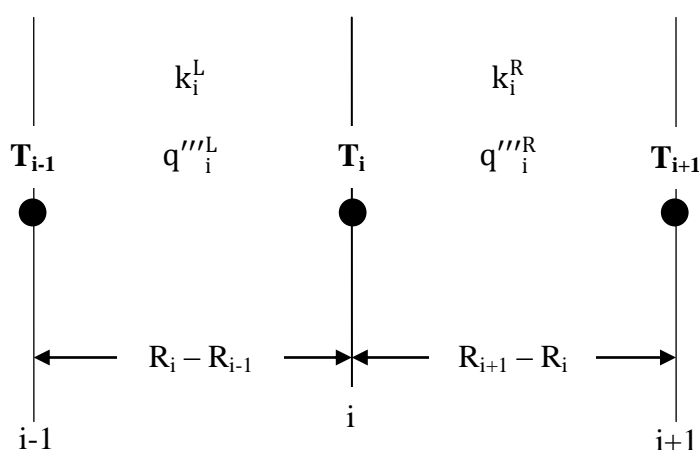


Figure 2: Mesh point layout

The spatial finite difference approximations use an exact expression for the volume associated with the power density and the surface area associated with the temperature gradient. For simplicity, the gradient approximation would be included in the definition of the surface area. In order to avoid writing unique expression for each geometry and to condense numerical expressions, the following quantities are defined:

$$\begin{aligned}
S_i^L &= (2\pi)^P \left(\frac{R_i + R_{i-1}}{2} \right)^P \left(\frac{1}{R_i - R_{i-1}} \right) & S_i^R &= (2\pi)^P \left(\frac{R_i + R_{i+1}}{2} \right)^P \left(\frac{1}{R_{i+1} - R_i} \right) \\
V_i^L &= (2\pi)^P \left(\frac{R_i - R_{i-1}}{2} \right) \left(\frac{3R_i + R_{i-1}}{4} \right)^P & V_i^R &= (2\pi)^P \left(\frac{R_{i+1} - R_i}{2} \right) \left(\frac{3R_i + R_{i+1}}{4} \right)^P \quad (3) \\
S_i^B &= (2\pi R_i)^P & P &= \begin{cases} 0, & \text{Rectangular geometry} \\ 1, & \text{Cylindrical geometry} \end{cases}
\end{aligned}$$

Where:

Superscripts, L and R, refer to Left and Right of node i, respectively.

R_i : Space coordinates at node i.

S_i^L : Surface area-gradient weight at the left of node i.

S_i^R : Surface area-gradient weight at the right of node i.

V_i^L : Volume at the left of node i.

S_i^B : Surface area at the exterior boundary.

P: Factor that is used to determine the type of geometry.

By expanding Eq.(1) into a finite difference form, it gives:

$$(T_i - T_{i-1})k_i^L S_i^L + (T_i - T_{i+1})k_i^R S_i^R = q''^L V_i^L + q''^R V_i^R \quad (4)$$

Rearranging Eq.(4) to be written in the following matrix format:

$$\begin{aligned}
& a_i T_{i-1} + b_i T_i + c_i T_{i+1} = d_i \\
a_i &= -k_i^L S_i^L & b_i &= -a_i - c_i & c_i &= -k_i^R S_i^R & d_i &= q''^L V_i^L + q''^R V_i^R \quad (5)
\end{aligned}$$

Eq.(5) is used to calculate the temperature profile inside a solid material. The temperature at the boundary nodes would be calculated using Eq.(1) and Eq.(2), to eliminate the additional node on the left or the right of the boundary node. The general form of a left and right boundary condition equations are given by Eq.(6) and Eq.(7), respectively.

$$\begin{aligned}
& a_i T_{i-1} + b_i T_i + c_i T_{i+1} = d_i \\
a_i &= 0 & b_i &= \frac{k_i^R \alpha S_i^B}{\beta} - c_i & c_i &= -k_i^R S_i^R & d_i &= \frac{k_i^R \gamma S_i^B}{\beta} + q''^R V_i^R \quad (6)
\end{aligned}$$

$$a_i T_{i-1} + b_i T_i + c_i T_{i+1} = d_i$$

$$a_i = -k_i^L S_i^L \quad b_i = \frac{k_i^L \alpha S_i^B}{\beta} - a_i \quad c_i = 0 \quad d_i = \frac{k_i^L \gamma S_i^B}{\beta} + q_i''' V_i^L \quad (7)$$

The thermal conductivity is considered to be a function of temperature and burnup, in case of a fissile mesh zone. The temperature that would be used to evaluate the thermal conductivity, or any thermal property, is the average temperature bounding each mesh interval, Eq.(8).

$$k_i^L = k_{i-1}^R = k \left(\frac{T_{i-1} + T_i}{2} \right) \quad k_i^R = k_{i+1}^L = k \left(\frac{T_i + T_{i+1}}{2} \right) \quad (8)$$

2.2 Thermal Properties.

The following thermal properties are needed to be able to calculate the temperature distribution: fuel and cladding thermal conductivity, coolant convective heat transfer coefficient, and gap conductance.

The fuel thermal conductivity is considered to be a function of temperature and burnup. The fuel thermal conductivity is applicable to UO₂, UO₂-Gd₂O₃ and MOX fuel (Geelhood and Luscher, 2011).

I. For UO₂ and UO₂-Gd₂O₃ fuel pellets:

$$k_{95} = \frac{1}{A + a * gad + BT + f(Bu) + [1 - 0.9 * e^{-0.04 * Bu}] * g(Bu) * h(T)} + \frac{E}{T^2} e^{-\frac{F}{T}} \quad (9)$$

II. For MOX fuel pellets:

$$K_{95} = \frac{1}{A(x) + a * gad + B(x)T + f(Bu) + [1 - 0.9 * e^{-0.04 * Bu}] * g(Bu) * h(T)} + \frac{C}{T^2} e^{-\frac{D}{T}} \quad (10)$$

Where:

k₉₅: Thermal conductivity for 95% of fuel theoretical density, (W/m.K).

T: Temperature, (K).

Bu: Burnup, (GWd/MTU).

f (Bu): Effect of fission products in crystal matrix = 0.00187*B_u

g (Bu): Effect of irradiation defects = 0.038*B_u^{0.28}

h (T): Temperature dependence of annealing on irradiation defects

$$h(T) = \frac{1}{1 + 396 * e^{-\frac{6380}{T}}} \quad a: 1.1599 \quad gad: \text{weight fraction of gadolinia (Unitless).}$$

A: 0.0452 (m.K/W)

C: 1.5E9 (W.K/m)

A(x): 2.85*x + 0.035 (m.K/W)

D: 13520 (K)

x: 2.00 – O/M, O/M: Oxygen-to-Metal atomic ratio

E: 3.5E9 (W.K/m)

B: 2.46E-04 (m/W)

F: 16361 (K)

B(x): (2.86 – 7.15*x)*1.0E-04 (m/W)

The Fuel thermal conductivity could be adjusted for as-fabricated fuel density (in fraction of theoretical density) (Geelhood and Luscher, 2011):

$$K_d = 1.0789 * K_{95} * \left(\frac{d}{1.0 + 0.5 * (1 - d)} \right) \quad (11)$$

Where:

d: Fraction of theoretical density (ratio of actual density to theoretical density).

The factor 1.0789 in Eq.(11) adjusts the conductivity back to that for 100 % theoretical density material. Limitation of the fuel thermal conductivity empirical formulas, Eq.(9) and Eq.(10), are as follows:

- a. Temperature: 300 to 3000K
- b. Rod-average burnup: 0 to 62 GWd/MTU
- c. As-fabricated density: 92 to 97 % theoretical density
- d. Gadolinia content: 0 to 10 wt%

The cladding thermal conductivity is considered as a function of temperature. The cladding thermal conductivity is applicable for Zircaloy-2, Zircaloy-4, ZIRLO, M5, ZrNb-1 and SS-304. The following correlations were used to predict cladding thermal conductivity:

- I. For Zircaloy-2, Zircaloy-4, ZIRLO and M5 (Hagrman and Reymann, 1979)

$$k_{\text{Zircaloy}} = A + BT + CT^2 + DT^3$$

A: 7.51 B: 2.09E-02 C: -1.45E-05 D: 7.67E-09 (12)

Where:

k_{Zircaloy} : thermal conductivity of Zircaloy (W/m.K) T: Temperature (K)

- II. For ZrNb-1 (Geelhood and Luscher, 2011):

$$K_{\text{ZrNb-1}} = A + BT + CT^2 + DT^3$$

A: 15.06 B: 6.96E-03 C: 1.61E-06 D: 2.47E-10 (13)

Where:

$k_{\text{ZrNb-1}}$: thermal conductivity of ZrNb-1 (W/m.K) T: Temperature (K)

- III. For AISI 304 Stainless steel (ASME, 1992)

$$k_{\text{SS}} = A + BT + CT^2 + DT^3$$

A: 8.95 B: 2.25E-02 C: -9.27E-06 D: 3.17E-09 (14)

Where:

k_{SS} : thermal conductivity of AISI 304 Stainless steel (W/m.K) T: Temperature (K)

The convective heat transfer coefficient is used in region interface between solid and liquid. The heat transfer from the solid surface (e.g. cladding) to the coolant would be governed only to a single phase forced convection.

The Dittus-Boelter correlation would be used for turbulent ($Re \geq 2300$) forced convection flow (Todreas and Kazimi, 1993):

$$h_f = \left(\frac{0.023 * k_c}{D_h} \right) * Re^{0.8} * Pr^{0.4} \quad (15)$$

The Sellars, Tribus, and Klein correlation would be used for laminar ($Re < 2300$) forced convection flow (Todreas and Kazimi, 1993):

$$h_f = \left(\frac{4.36 * k_c}{D_h} \right) \quad (16)$$

Where:

h_f : Convective heat transfer coefficient ($W/m^2.K$)	ρ_c : Coolant density (Kg/m^3)
k_c : Coolant thermal conductivity ($W/m.K$)	V_{inlet} : Inlet velocity (m/s)
D_h : Hydraulic diameter (m)	μ_c : Dynamic viscosity ($Kg/m.s$)
Re: Reynolds number	$Re = \frac{\rho_c * V_{inlet} * D_h}{\mu_c}$
Pr: Prandtl number	$Pr = \frac{C_p * \mu_c}{k_c}$
C_p : Specific heat capacity ($J/Kg.K$)	

All coolant properties needed to calculate the convective heat transfer coefficient are evaluated at coolant bulk temperature.

The gap conductance is the sum of two components: the conductance due to radiation and the conduction through the gas. Radiation-induced swelling and thermal expansion in fuel pellet resulting in a contact between pellets and cladding is ignored. Hence, the conduction through regions of solid-solid contact is ignored. The considered gap conductance model is called open-gap model, which is presented as follows (Geelhood, Luscher and Beyer, 2011):

$$h_{gap} = h_{rad} + h_{gas} \quad (17)$$

Where:

h_{gap} : Gap conductance ($W/m^2.K$)
h_{rad} : Conductance due to radiation ($W/m^2.K$)
h_{gas} : Conductance of the gas gap ($W/m^2.K$)

The radiation heat transfer occurs between two separated surfaces with different surface temperatures. The conductance due to radiation heat transfer is expressed by the following equation (Geelhood, Luscher and Beyer, 2011):

$$h_{\text{rad}} = \sigma * F * \underbrace{(T_i^2 + T_{i+1}^2) * (T_i + T_{i+1})}_{\text{if Solid - Gap interface}} = \sigma * F * \underbrace{(T_{i-1}^2 + T_i^2) * (T_{i-1} + T_i)}_{\text{if Gap - Solid interface}} \quad (18)$$

Where:

σ : Stefan-Boltzmann constant = 5.6697E-08 (W/m².K⁴)

$$F: \text{View factor} = \frac{1}{E_B + \left(\frac{r_B}{r_C}\right) \left(\frac{1}{E_D - 1}\right)}$$

E_B : Cladding surface emissivity.

r_B : Inner cladding radius (m).

E_D : Fuel surface emissivity.

r_C : Fuel radius (m).

The conduction through gas gap is a function of gas thermal conductivity and gap effective width. Fuel and cladding thermal expansion effect on gap width is ignored. As well, the temperature jumps distance. The conduction through gas gap is expressed as following (Geelhood, Luscher and Beyer, 2011):

$$h_{\text{gas}} = \frac{k_{\text{gas}}}{\Delta r} \quad (19)$$

Where:

k_{gas} : Gas thermal conductivity (W/m.K).

Δr : Gap width (m).

The gas thermal conductivity is considered to be a function of temperature and gas atomic fraction in the gap for any of the seven gases: He, Ar, Kr, Xe, H₂, N₂ and steam.

2.3 Solution Methodology.

The finite difference equations in the matrices form (Eq.(5), Eq.(6) and Eq.(7)) lead to a tridiagonal matrix whose diagonal (b_i) is positive and greater than the sum the magnitude of the off-diagonal elements (a_i and c_i).

The iteration procedure begins first with a guess temperature per radii in order to find thermal properties. Then, the temperature profile is calculated using the Eqs.(5), (6) and Eq.(7). Finally, repeating these procedures until achieving the user defined-convergence criteria at the central node or the maximum number of iteration (see Figure 3)

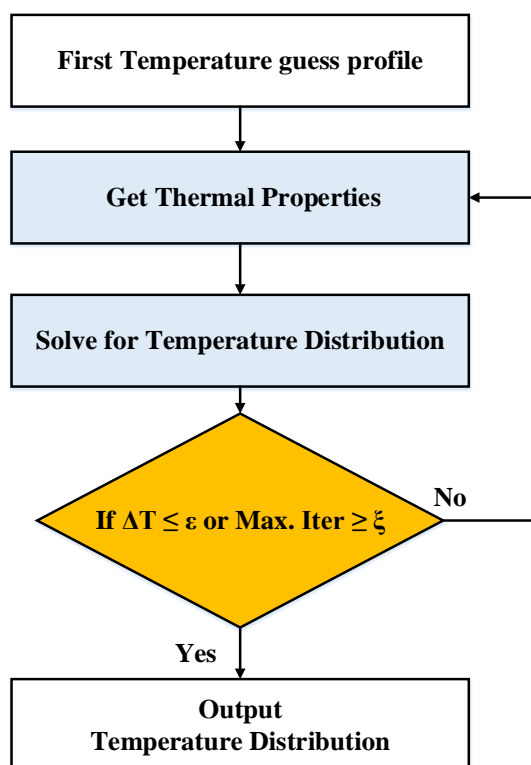


Figure 3: Flowchart of the thermal-hydraulic model

2.4 Neutronic – Thermal-Hydraulic Feedback

CONDOR (Villarino, 2002) is a cell neutronic calculation code developed by INVAP's Nuclear Engineering Department. CONDOR uses either a collision probability method or heterogeneous response method to solve the neutronic flux in a multi-group scheme.

The neutronic – thermal-hydraulic feedback scheme is accomplished using the following steps: First, CONDOR is used to generate power density per mesh with a guessed flat temperature for each material (Fuel, Cladding, and Coolant). Second, the generated power density is fed to the thermal-hydraulic model in order to get the temperature distribution per radii; this step is repeated till reaching the temperature convergence criteria. Third, the converged temperature profile is sent back to CONDOR to correct the power density. Finally, this step is repeated until reaching a convergence in the power density. Figure 4 illustrates the feedback scheme.

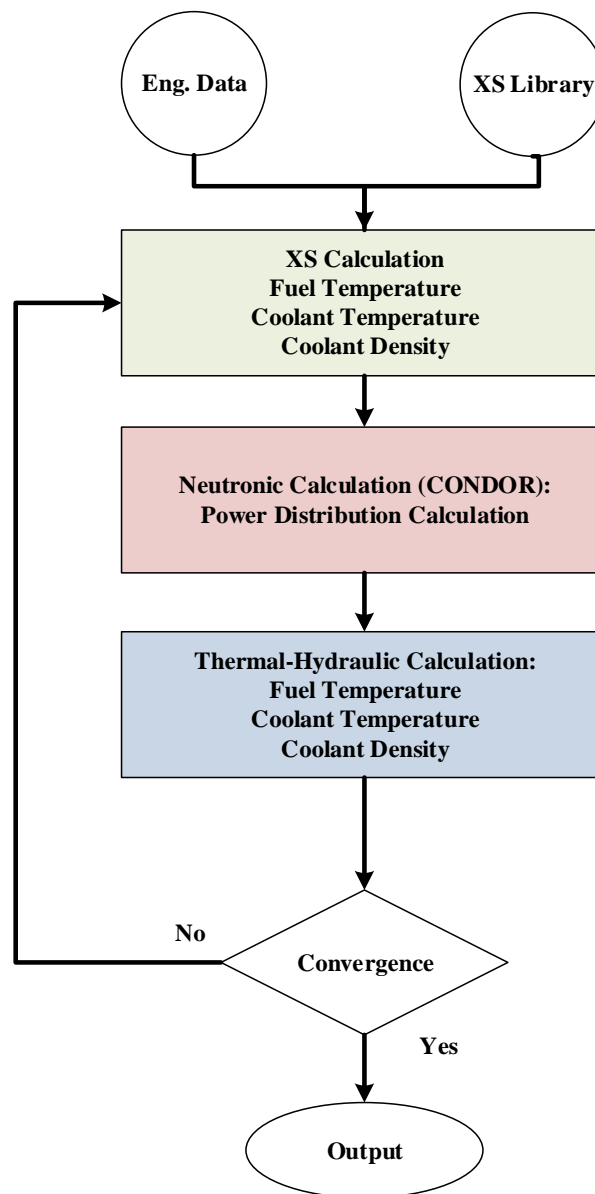


Figure 4: Neutronic – Thermal-hydraulic feedback scheme

3 VERIFICATION AGAINST AN ANALYTICAL PROBLEM

Verification is concerned with identifying and removing errors in the model by comparing numerical solutions to analytical or highly accurate benchmark solutions. The analytical problem 3.98 from (Bergman, Lavine, Incropera and Dewitt, 2011) has been selected to compare the analytical solution with the numerical solution.

The analytical problem is about a nuclear reactor fuel pin with (6 mm) radius of UO_2 and (3 mm) thick cladding. The thermal conductivity for the fuel and cladding is (2 W/m.K) and (25 W/m.K), respectively. A uniform heat generation occurs in the fuel region with a power density equal to $(2.0 \times 10^8 \text{ W/m}^3)$. The outer surface of the cladding is exposed to a coolant that is characterized by a temperature (300K) and a convection heat transfer coefficient (2000 W/m².K).

Ten equispaced nodes were used to solve the previous problem. Table 1 presents the analytical and numerical results.

i	R _i (m)	Temperature at node i (K)		Difference in Temp. between Analytical and Numerical Solution (K)	Zone
		Analytical Solution	Numerical Solution		
0	0.00E+00	1458.39	1458.30	-0.09	Fuel
1	1.00E-03	1433.39	1433.30	-0.09	
2	2.00E-03	1358.39	1358.30	-0.09	
3	3.00E-03	1233.39	1233.30	-0.09	
4	4.00E-03	1058.39	1058.30	-0.09	
5	5.00E-03	833.39	833.30	-0.09	
6	6.00E-03	558.39	558.30	-0.09	
7	7.00E-03	536.19	536.14	-0.05	Cladding
8	8.00E-03	516.96	516.94	-0.02	
9	9.00E-03	500.00	500.00	0.00	

Table 1: Comparison between analytical and numerical solution

A good agreement was found between the analytical and numerical solutions. It can be noted from Table 1 at node 9, which is located at the cladding outer surface, that there is no difference in temperature. This is because of the use of an exact equation in the numerical model at solid-coolant interfaces. This equation satisfies that the outgoing heat flux from the rod surface is equal to the product of the coolant convective heat transfer coefficient with the difference in temperature between the cladding surface and bulk temperature.

4 CASE STUDY: TYPICAL PWR FUEL PIN

The specification of a typical PWR fuel pin (Todreas and Kazimi, 1993) is provided in Table 2. The power density was generated using CONDOR for a first uniform temperature guess of: fuel (700 K), cladding (560K) and coolant (560 K).

Coolant inlet temperature (°C)	292.7
Average temperature rise in the reactor (°C)	33.4
Convective heat transfer coefficient (W/m ² .K) (Calculated using a typical PWR coolant velocity)	34,000
Fuel pellet diameter (mm)	8.19
Fuel rod diameter (mm)	9.5
Fuel material	UO ₂ – 3.23 % of enrichment
Fuel rod pitch (mm)	12.6
Cladding thickness (mm)	0.57
Cladding material	Zircaloy-4
Fuel density (g/cm ³)	10.126

Table 2: Typical PWR specification.

Using CONDOR, 5 meshes were used at the fuel zone, and a single mesh for both the gap and cladding zones. The normalized power density based on the first uniform guessed temperatures for a 0 and 80 GWd/Tn burnup is presented in Figure 5.

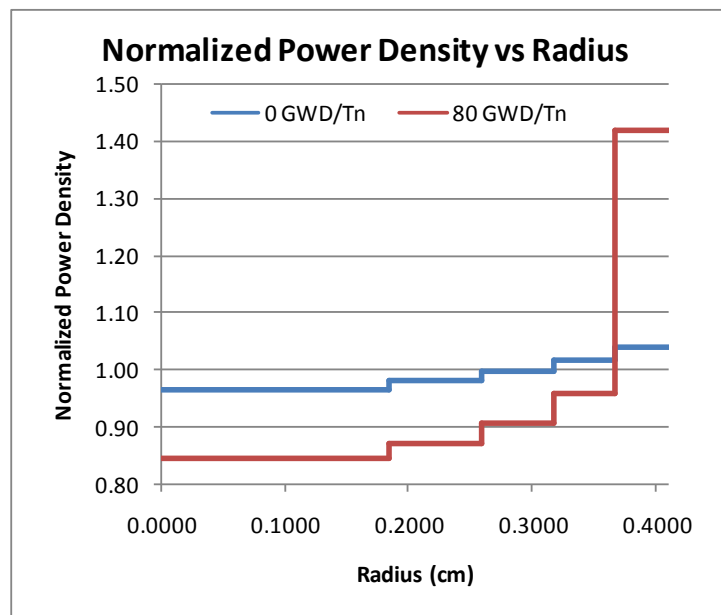


Figure 5: Normalized power density at burnup of 0 and 80 GWd/Tn of a typical PWR fuel pin using CONDOR code.

The previous information was used as an input to the thermal-hydraulic model. The convergence criteria were set to be 0.1 K. The temperature profiles for the typical PWR fuel pin at fresh loading and 80 GWd/Tn rod-average burnup are presented in Figure 6.

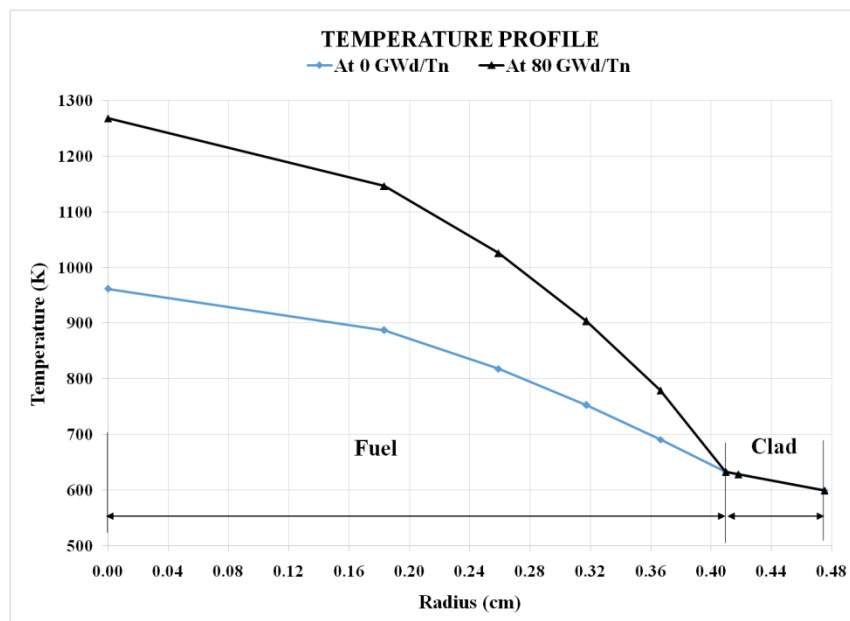


Figure 6: Temperature distribution at 0 and 80 GWd/Tn in a typical PWR fuel pin using the thermal-hydraulic model.

In this case study, the convergence criteria was met after five iterations. It can be noticed from Figure 6 that the average fuel temperature per mesh at fresh loading was 925, 853, 785, 722 and 662 K. And, at an average fuel burnup of 80 GWd/Tn was 1207, 1086, 965, 841 and 706 K. The average cladding temperature was at 620 K. The coolant bulk temperature was at 582 K. Using these average temperatures into CONDOR code, yield the following power density distribution (Table 3 and Table 4).

	Normalized Power Density at 0 GWd/Tn Burnup				
	Mesh 1	Mesh 2	Mesh 3	Mesh 4	Mesh 5
First guess (Uniform temperatures)	0.967	0.980	0.996	1.016	1.041
Calculated temperature profile	0.968	0.980	0.997	1.016	1.039
Reactivity difference after correcting the temperatures	246 pcm				

Table 3: Comparison in the normalized power density at fresh loading between the uniform guess and the calculated temperatures profile.

	Normalized Power Density at 80 GWd/Tn Burnup				
	Mesh 1	Mesh 2	Mesh 3	Mesh 4	Mesh 5
First guess (Uniform temperatures)	0.845	0.871	0.906	0.958	1.420
Calculated temperature profile	0.845	0.871	0.906	0.958	1.420
Reactivity difference after correcting the temperatures	447 pcm				

Table 4: Comparison in the normalized power density at 80 GWd/Tn average burnup between the uniform guess and the calculated temperatures profile.

It can be noted from [Table 3](#) and [Table 4](#) that the temperature changes at 80 GWd/Tn burnup has a higher impact on the reactivity feedback than at fresh loading. This result provides a better prediction for the in-core fuel management, which has an influence on the reactor operation.

5 CONCLUSION AND FUTURE WORK

A thermal-hydraulic model has been developed, verified and tested. It has been developed to solve pin-by-pin the temperature distribution for a steady state non-uniform mesh interval, power density and thermal conductivity. Thermal properties could be a user defined value or a built-in formula. Fuel thermal conductivity built-in formula was considered to be a function of temperature and burnup. A set of cladding thermal conductivities formulas were considered to be a temperature-dependent 3rd degree polynomial.

A verification process was carried out to examine the numerical model. A good agreement was found between the analytical and the numerical solution with a maximum difference in temperature equal to 0.1 K (0.01%). A case study of a typical PWR fuel pin was accomplished with the aid of CONDOR code, which provided the power density and burnup distribution. This case study is considered a first step in coupling the thermal-hydraulic model with CONDOR code.

Further tests are required to ensure the reliability and to increase the confidence level of the thermal-hydraulic model. Verification against a well-developed thermal-hydraulic code such as RELAP would be an advantage. Upon a successful verification tests, the thermal-hydraulic model will be internally coupled to CONDOR code.

REFERENCES

- ASME, ASME Boiler and Pressure Vessel Code, Section II – Materials, Part D, Properties, the American Society of Mechanical Engineers, New York, 1992.
- Bergman, T.L., Lavine, A.S., Incropera F.P. and Dewitt, D.P. “Fundamentals of Heat and Mass Transfer”. John Wiley & Sons, 2011.
- E. Villarino, “CONDOR Calculation Package”, International Conference on the New Frontiers of Nuclear Technology: Reactor Physics, Safety and High-Performance Computing. Physor 2002, Seoul, Korea, October 7-10, 2002.
- Geelhood, K.J. and Luscher, W.G. “Material Property Correlations: Comparisons between FRAPCON-3.4, FRAPTRAN 1.4, and MATPRO”. Tech. Rep. NUREG/CR-7024. Pacific Northwest National Laboratory, March 2011.
- Geelhood, K.J., Luscher, W.G. and Beyer, C.E. “FRAPCON-3.4: A Computer Code for the Calculation of Steady-State Thermal-Mechanical Behavior of Oxide Fuel Rods for High Burnup”. Tech. Rep. NUREG/CR-7022, Vol. 1. Pacific Northwest National Laboratory, March 2011.
- Hagrman, D.L. and Reymann, G.A. “MATPRO-Version 11: A Handbook of Materials Properties for Use in the Analysis of Light Water Reactor Fuel Rod Behavior”. Tech. Rep. NUREG/CR-0497. Idaho National Engineering Laboratory, February 1979.
- Todreas, N.E. and Kazimi, M.S. “Nuclear System I: Thermal Hydraulic Fundamentals”. Taylor & Francis publishers, 1993.